

Experimental model for a DMC-based control applied to a PEM Fuel Cell

Diego Feroldi, Miguel Allué, Jordi Riera, Maria Serra and Marta Basualdo

Abstract—This paper addresses the control of an experimental PEM fuel cell system. The fuel cell station is composed by an ElectroChem[®] 7-cell stack with Nafion 115[®] membrane electrodes assemblies (MEAs) and the auxiliary equipment. The control problem is focussed on the air supply in the cathode. The main objectives are to regulate the stack voltage and the cathode oxygen excess ratio. The manipulated variables are the compressor motor voltage and the command current of a proportional valve located at the cathode outlet. A linear and dynamic model at a given operational point is obtained via step tests, which is used in the context of a centralized multivariable Dynamic Matrix Control (DMC).

I. INTRODUCTION

PEM fuel cell technology is a promising alternative for electrical energy generation in a wide spectrum of applications, from low power ones such as portable electronics to high power ones such as electric vehicles or stand-alone residential applications. The dynamic behavior and the generated power in a fuel cell system depend on the control of the system. When a load is connected to the fuel cell, the control system must control the temperature, the membrane hydration and the partial pressure of gases at both sides of the membrane to avoid voltage degradation and, therefore, a reduction in the efficiency [1]. Besides, it is important to control properly the mentioned variables to assure the durability of the cells. These critical variables must be controlled for a wide range of power, with a series of actuators such as valves, pumps, compressors, expanders, fans, humidifiers and condensers.

For several reasons, including the system efficiency and the need to avoid oxygen starvation, the control problem on the cathode air supply is receiving a significant attention in the literature [2]. Focused on this problem, this paper presents a control structure with a regulating valve for the cathode outlet flow in combination with the compressor motor voltage as manipulated variables in a fuel cell system. The influence of these input variables have already been studied in detail in [2] and here are exploited to implement a predictive control strategy based on dynamic matrix control

(DMC) in an experimental fuel cell test station. The objectives of this control strategy are to regulate both the fuel cell voltage and the oxygen excess ratio in the cathode.

The oxygen excess ratio (λ_{O_2}) is a parameter that indicates the excess of oxygen in the cathode, which is defined as

$$\lambda_{O_2} = \frac{W_{O_2, in}}{W_{O_2, rct}}, \quad (1)$$

where $W_{O_2, in}$ is the cathode inlet oxygen mass flow (measured variable) and $W_{O_2, rct}$ is the reacting oxygen mass flow in the cathode electrochemical reaction. This last flow depends on the stack current I_{fc} (measured variable):

$$W_{O_2, rct} = M_{O_2} \frac{n I_{fc}}{4 F}, \quad (2)$$

where $M_{O_2} = 32 \times 10^{-3} \text{ kg mol}^{-1}$ is the molar mass of oxygen, $n = 7$ is the stack cell number, and $F = 96485 \text{ C mol}^{-1}$ is the Faraday number.

This paper is organized as follows. In Section II, a detailed description of the fuel cell test station is presented. Section III presents the fuel cell system model considered for control design. Section IV explains the DMC strategy. In Section V, the most relevant results obtained from the implementation of the controller designed are presented. Finally, the main conclusions and some lines of further research are exposed in Section VI.

II. DESCRIPTION OF THE FUEL CELL TEST STATION

The principal components of the fuel cell test station are a fuel cell stack, an air compressor, a hydrogen storage tank, gases manifolds, humidifiers, line heaters and valves. The simplified schematic diagram in Fig. 1 shows the main components of the fuel cell experimental setup and Table I presents the description of each measured and controlled variable. Other variables, for example the temperature and the individual voltage of each cell, are also measured for monitoring purposes but not shown in the schematic diagram for clarity. Additionally, Fig. 2 shows the real fuel cell test station.

The fuel cell stack is an ElectroChem[®] 7-cell stack with Nafion 115[®] membrane electrodes assemblies (MEAs), with a catalyst loading of 1 mg cm^{-2} of platinum, 50 cm^2 of active area, 50 W of nominal power and 100 W of peak power. The membrane exchange humidifiers used to maintain proper humidity conditions inside the cells are Cellkraft[®]. The air compressor consists in a 12 V DC oil-free diaphragm vacuum pump. The temperature of the line heaters and

This work was supported by the project PICT 2009-0017 of the ANPCyT (Argentina), and the projects DPI2010-15274 and DPI 2011-25649 (Spain).

D. Feroldi is with CAPEG-CIFASIS-(CONICET-UNR-AMU) and DCC-FCEIA-UNR, 27 de Febrero 210 bis, S2000EYP Rosario, Argentina, feroldi@cifasis-conicet.gov.ar

M. Allué, J. Riera and M. Serra are with IRI-(CSIC-UPC), Llorens i Artigas 4-6, 08028 Barcelona, Spain, mallue/riera/maserra@iri.upc.edu

M. Basualdo is with CAPEG- CIFASIS-(CONICET-UNR-AMU) and Chem. Eng. Dpt. FRRo-UTN, 27 de Febrero 210 bis, S2000EYP Rosario, Argentina basualdo@cifasis-conicet.gov.ar

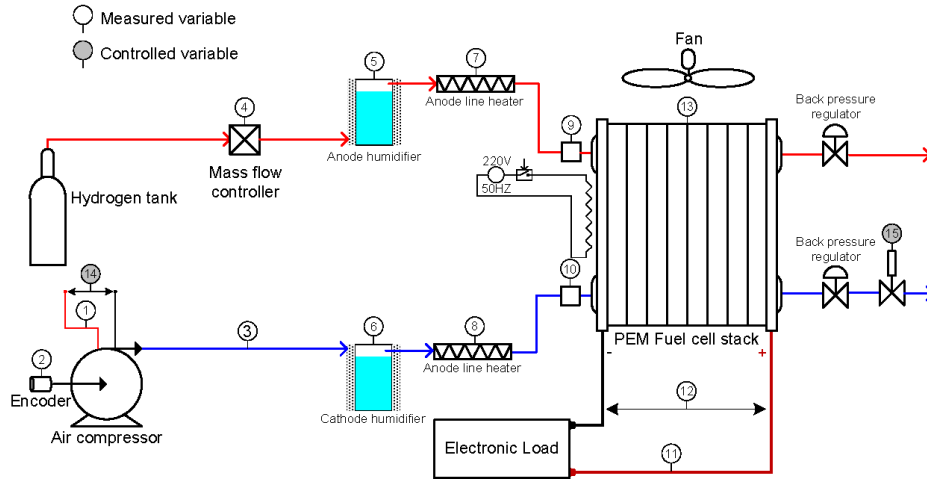


Fig. 1. Simplified schematic diagram of the fuel cell test station. Variables names are in Table I.

TABLE I
MEASURED AND CONTROLLED VARIABLES IN THE FUEL CELL TEST STATION

N ^o	Variable name	Type
1	Compressor motor current I_{cm} (A)	Measured
2	Compressor Rotational speed ω_{cp} ($rad\ s^{-1}$)	
3	Cathode mass flow rate W_{ca} ($kg\ s^{-1}$)	
4	Anode mass flow rate W_{an} ($kg\ s^{-1}$)	
5	Anode humidifier temperature $T_{hum,an}$ ($^{\circ}C$)	
6	Cathode humidifier temperature $T_{hum,ca}$ ($^{\circ}C$)	
7	Anode line heater temperature $T_{ln,an}$ ($^{\circ}C$)	
8	Cathode line heater temperature $T_{ln,ca}$ ($^{\circ}C$)	
9	Anode Pressure P_{an} (Bar)	
10	Cathode Pressure P_{ca} (Bar)	
11	Stack current I_{st} (A)	
12	Stack voltage V_{st} (V)	
13	Stack temperature T_{st} ($^{\circ}C$)	
14	Compressor motor voltage V_{cm} (V)	
15	Valve command current I_{valve} (mA)	

the stack temperatures are controlled by decentralized PID controllers, allowing independent settings of gas conditions (humidity and temperature) inside the stack [3].

The data acquisition and control system is composed by a *Host* computer and a computer running in real time, namely *RTOS* computer. The *RTOS* computer communicates with the input/output (I/O) modules, made by *National Instrument*[®], throughout a *FPGA* target and a *PCI* bus. The two computers are connected via ethernet. The *Host* computer also allows monitoring the evolution of the system variables and commanding the system through a graphical interface developed in *LabVIEW*[®]. An extensive amount of variables (the main listed in Table I) are measured and recorded every 100 *ms*.

The controlled valve located at the cathode output is a *Bürkert*[®] proportional valve Type 2822 with an orifice of 0.8 *mm*. The valve control is done through the control electronics of Type 8605, which converts an analogous input signal into a Pulse-Width Modulated (PWM) signal. The input signal, which is one of the two control variables later used in the control strategy, is a current from 0 to 20 *mA*.

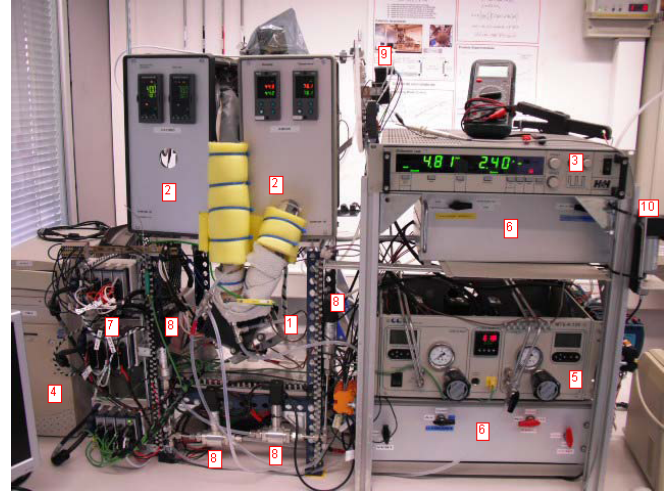


Fig. 2. Fuel cell test station at IRI (CSIC-UPC). 1: Fuel cell stack; 2: humidifiers; 3: electronic load; 4: real-time computer; 5: back-pressure regulators; 6: valves; 7: acquisition and control cartridges; 8: pressure sensors; 9: cathode outlet proportional valve; 10: air compressor.

With the input signal at zero, the valve closes tightly. Notice that in the real setup the current required to open the valve completely is 21 *mA*, slightly higher than the nominal value (20 *mA*).

The operation at a higher pressure increments the generated voltage as a result of the increment in the cathode oxygen partial pressure and the anode hydrogen partial pressure:

$$E = 1.229 - 0.85 \times 10^{-3}(T_{fc} - 298.15) + 4.3085 \times 10^{-5}T_{fc}[\ln(p_{H_2}) + 0.5\ln(p_{O_2})], \quad (3)$$

where E is the open circuit voltage of each single cell in volts, T_{fc} the fuel cell temperature in Kelvin and p_{H_2} and p_{O_2} are the anode partial pressure of hydrogen and cathode partial pressure of oxygen, respectively, in atm. In Fig. 3, two

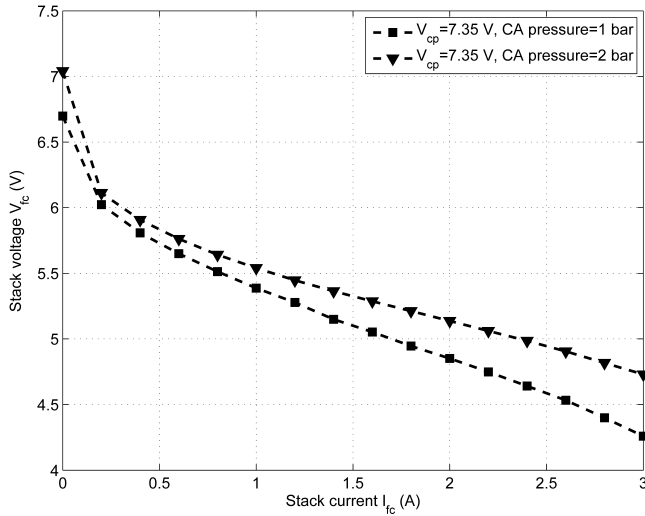


Fig. 3. Polarization curves at different cathode pressures (closing the outlet valve).

polarization curves at different cathode pressures (closing the outlet valve) are presented to show the influence of the cathode pressure in the stack voltage.

The compressor motor voltage as a control input allows regulating the oxygen partial pressure in the cathode. Augmenting the compressor voltage the oxygen partial pressure increases. In fact, the only variable used to control the air supply in the cathode, from the literature review, is the compressor motor voltage [1], [4], [5], [6], [7].

However, in [2] it is proposed the use of a proportional valve at the cathode output. This new variable regulates the outlet air flow in conjunction with the compressor motor voltage. In fact, a diminution of the area of the valve that closes the cathode air flow contributes to increase the cathode pressure and, at the same time, contributes to decrease the air flow, the stoichiometry, and the oxygen concentration [2]. Fig. 4 shows the increment in the cathode pressure when the valve is closing from fully open ($I_{valve} = 21 \text{ mA}$) to partial openings. Thus, one of the main advantages of this control structure is that it allows to regulate both the fuel cell voltage and oxygen excess ratio in the cathode.

III. MATHEMATICAL MODEL

Mathematical models experimentally validated provide a powerful tool for the development and improvement of fuel cell-based systems. Mathematical models can be used to describe the fundamental phenomena that take place in the system, to predict the behavior under different operating conditions and to design and optimize the control of the system. Most of the empirical models, such as [8], [9], [10], are focused in the prediction of the polarization curve, which is used to characterize the electrical operation. Nevertheless, in spite of having many models that study the cells in stationary state, there are few dynamic models suitable for control purposes like [1].

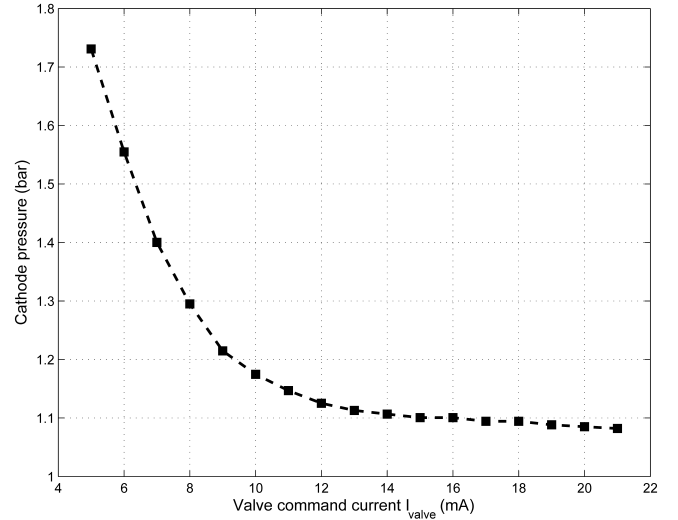


Fig. 4. Cathode pressure for different valve openings. When $I_{valve} = 21 \text{ mA}$ the valve is fully open.

Due to the complexity of a model representing the non-linear behavior of the system, the model-based controller proposed in this article is designed through step response tests at a given equilibrium point. The models based on step response are one of the most used in the academic literature of predictive control and in some commercial products.

The step-response models are constructed applying a step signal to each input (manipulated variable or actuator) of the plant, and recording the open-loop response of each output variable, until all the output variables have settled to constant values [11]. If the assumed model is linear, knowing the step response allows to deduce the response to any other input signal.

Therefore, the predicted response of the output j to the vector of M inputs u , truncated using N values, is given by:

$$\hat{y}_j(t+k|k) = \sum_{m=1}^M \sum_{i=1}^N s_i^{mj} \Delta u_m(t+k-i|t) \quad (4)$$

where s_i^{mj} are the sampled output values of the output j for the step input m and $\Delta u_m(t) = u_m(t) - u_m(t-1)$.

Here, three step response tests were conducted, each one exciting a different input with the others fixed. The first two inputs correspond to the two manipulated variables: the compressor motor voltage and the valve command current. The third input corresponds to the stack current, which is a measured disturbance. The first input u_1 is applied at time $t = 2709 \text{ s}$, u_2 is applied at $t = 632.4 \text{ s}$, and u_3 is applied at $t = 5452 \text{ s}$. In each test it is recorded the open-loop response of each output variable: the stack voltage and the oxygen excess ratio. Therefore, the six different step responses shown in Fig. 5 are collected. The step responses are normalized according to

$$s_i^{mj} = \frac{y_j(i) - y_j(0)}{\Delta u_m}, \quad (5)$$

where $y_j(i)$ is the j output response to the amplitude of the input step Δu_m applied in the m input and $y_j(0)$ is the output j in the instant when the step m is applied.

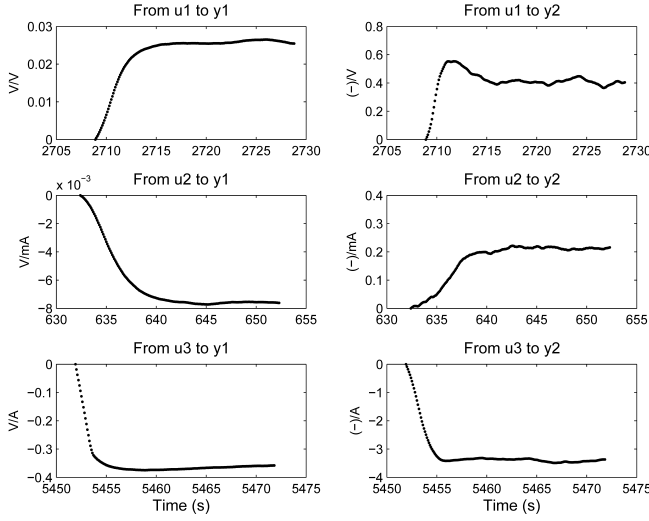


Fig. 5. Normalized step responses of the experimental outputs according to (5) when a step is applied in each input with the others fixed. The sampling time is 100 ms.

IV. CONTROL STRATEGY

A. Interaction analysis

The advantages of using the outlet valve area together with the compressor voltage will be exploited implementing a control strategy. First, a preliminary study about the interaction degree between the controlled and the manipulated variables could be done through the use of the Relative Gain Array (RGA). Even though it is well-known and has a widespread industry applications, some limitations are recognized. Based on this, several new extensions of the RGA have appeared in the literature. A deep analysis of the different variants for RGA can be found in [12].

Therefore, an analysis of interaction using the RGA is done in this section. The RGA is the ratio of the *open loop* and *closed loop* gains, and can be computed as

$$RGA = G_\lambda \times (G_\lambda^{-1})^T, \quad (6)$$

where \times denotes element-by-element multiplication and G_λ is the gain matrix of the system. Each element of the gain matrix, g_{ij} , is the steady-state gain of output y_j when the control input u_i is altered but the other input is kept constant:

$$G_\lambda = \begin{bmatrix} \left. \frac{\Delta V_{fcs}}{\Delta V_{cm}} \right|_{I_{valve}^0} & \left. \frac{\Delta V_{fcs}}{\Delta I_{valve}} \right|_{V_{cm}^0} \\ \left. \frac{\Delta \lambda_{O_2}}{\Delta V_{cm}} \right|_{I_{valve}^0} & \left. \frac{\Delta \lambda_{O_2}}{\Delta I_{valve}} \right|_{V_{cm}^0} \end{bmatrix}. \quad (7)$$

In this analysis, the nominal values are: $I_{fc}^0 = 2 A$, $V_{cm}^0 = 5 V$, and $I_{valve}^0 = 14 mA$. The magnitude of the step in the inputs are: $\Delta I_{valve} = -3.5 mA$ and $\Delta V_{cm} = 1 V$. Thus, the resulting RGA matrix is

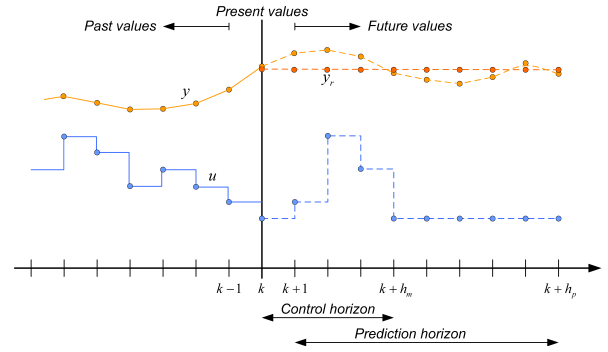


Fig. 6. Predictive control strategy

$$RGA = \begin{bmatrix} 0.642 & 0.358 \\ 0.358 & 0.642 \end{bmatrix}. \quad (8)$$

Analyzing the resulting RGA matrix, can be concluded that the interaction degree for this system would deteriorate the performance of a decentralized control. On the other hand, the interaction effect not always deteriorates the performance of the controlled process. It depends on the specifics plant objectives [13]. Therefore, in this preliminary study it seems convenient the use of a centralized multivariable controller, which avoids pairing variables, to resolve efficiently the interaction problem between the manipulated and the controlled variables.

B. Dynamic Matrix Control

The *Dynamic Matrix Control (DMC)* is a particular type of predictive control strategy that uses the step response to determine the so-called *Dynamic Matrix G* [14]. This matrix takes into account only the h_p first samples until the response tends to a constant value, assuming that the process is asymptotically stable, to predict the output as

$$y = G u + f, \quad (9)$$

where y is the time-vector of predicted outputs [2].

The control vector u is the sequence of future control actions and f is the free response vector, meaning that the response does not depend on future control movements. A graphical description of a general *predictive control strategy* can be seen in Fig. 6.

The dynamic matrix G is constructed from the coefficients obtained from the step response with prediction horizon h_p and control horizon h_m :

$$G = \begin{bmatrix} G_{11} & G_{12} \\ G_{21} & G_{22} \end{bmatrix}, \quad (10)$$

where each submatrix G_{ij} , of dimension $h_p \times h_m$, contains the values of the step response of the i -th output correspond-

ing to the j -th input:

$$G_{ij} = \begin{bmatrix} g_1 & 0 & \cdots & 0 \\ g_2 & g_1 & \cdots & 0 \\ \vdots & \vdots & \ddots & \vdots \\ g_{h_m} & g_{h_m-1} & \cdots & g_1 \\ \vdots & \vdots & \ddots & \vdots \\ g_{h_p} & g_{h_p-1} & \cdots & g_{h_p-h_m+1} \end{bmatrix}. \quad (11)$$

The objective of the *DMC* controller is to minimize the difference between the references y_{r_1} and y_{r_2} , and the predictions of the process outputs y_1 and y_2 over a horizon h_p in a least square sense with the possibility of including a penalty term for large control signal movements:

$$\min_u J(k). \quad (12)$$

The cost function $J(k)$ is defined as

$$J(k) = \sum_{j=1}^{h_p} [y(k+j|k) - y_r]^T R [y(k+j|k) - y_r] + \sum_{j=0}^{h_m} [\Delta u(k+j|k)]^T Q [\Delta u(k+j|k)], \quad (13)$$

where $\Delta u(k+j|k) \triangleq u(k+j|k) - u(k-1+j|k)$, R is a diagonal matrix to compensate the different ranges of values of the process outputs with diagonal elements r_1 and r_2 , and Q is also a diagonal matrix that allows to penalize the control effort with diagonal elements q_1 and q_2 . The parameters r_1 and r_2 affect the outputs y_1 and y_2 , respectively. Analogously, q_1 and q_2 affect the control inputs u_1 and u_2 , respectively.

If there are no restrictions in the manipulated variables, the minimization of the cost function $J(k)$ can be realized making its derivative equal to zero, resulting

$$\Delta u = (G^T R G + Q)^{-1} \cdot G^T \cdot R \cdot e, \quad (14)$$

where e is the vector of future errors along the prediction horizon.

However, as in all the predictive control strategies, only the first element of each calculated control sequence Δu is applied to the plant and, in the next sampling time, the sequence of control is calculated again using actualized information from the plant. For more details see [2].

V. RESULTS

The control horizon, the prediction control, the sampling time and the elements of the diagonal matrices R and Q were adjusted to achieve an adequate dynamic behavior of the fuel cell system. The values of R and Q have a strong influence on the transient response obtained. This is especially true for the weight matrix Q , which reduces the control effort. The higher are the values in Q , the lower is the control effort, but the response time is greater. The values chosen for these parameters after a systematic process of adjustment are shown in Table II.

TABLE II
PARAMETERS USED IN THE DMC CONTROLLER

Parameter	Value
Sampling time T_s	100 ms
Prediction horizon p	50
Control horizon m	5
Weight coefficient q_1	10
Weight coefficient q_2	30
Weight coefficient r_1	0.4
Weight coefficient r_2	0.7

The simulation results of the controlled system with variations in the load current according to the profile shown in Fig. 7(a) are presented: Fig. 7(b) shows the behavior of the controlled variables (λ_{O_2} and V_{fc}), while Fig. 7(c) shows the behavior of the manipulated variables (V_{cm} and I_{valve}).

As can be observed in the figures, the implemented controller has a good disturbance rejection: the stack voltage response has a maximum peak of 4.48% for a variation of 20% in the stack current I_{fc} at time $t = 1000$ s, while the oxygen excess ratio variation for the same I_{fc} variation is a narrow 14.95% peak.

It is remarkable that the control algorithm implements a compensation mechanism to rectify the inevitable model errors and deals with non-measured disturbances. This compensation mechanism utilizes measured output values, and thus, assures zero error at steady-state. It is also remarkable that controller testing shows a good performance in a wide operating range around the linearization point despite the internal controller model is linear.

VI. CONCLUSIONS AND FUTURE WORKS

This article proposes a control strategy based on predictive control (DMC) for a fuel cell system that uses the compressor motor voltage together with the cathode air flow valve area as manipulated variables. The controlled variables are the stack voltage and the oxygen excess ratio. To predict the future process response, the control strategy makes use of a process model that is easily obtainable through step response.

The simulation analysis of the DMC controller with the model obtained through experimental step tests shows an appropriate dynamic response. The control objectives has been accomplished with reduced control effort. This effort can be further reduced modifying the values of the matrix Q . This is particularly important because of practical limitations in the manipulated variables.

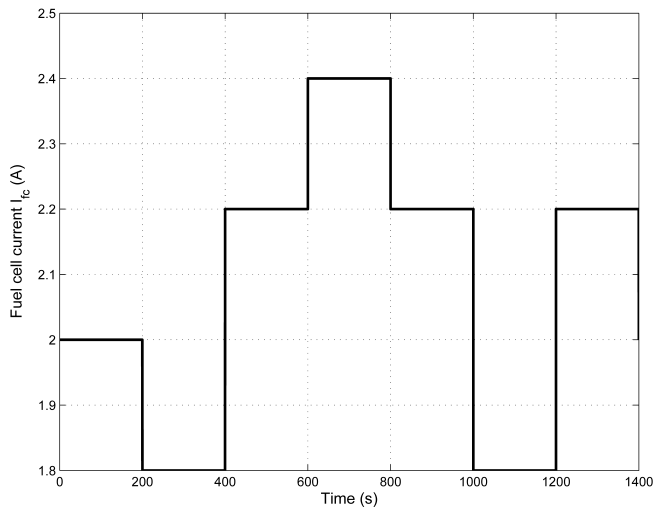
The results presented in this article provide a first step toward the implementation of the DMC-based controller working on-line in the test station, which is the final objective to validate completely the proposed control strategy.

VII. ACKNOWLEDGMENTS

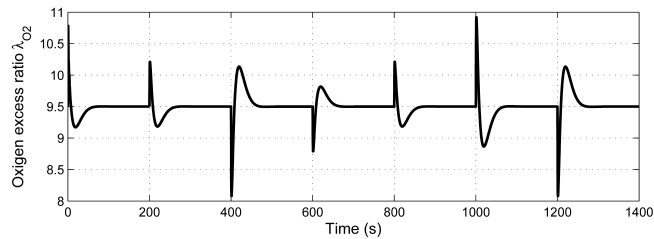
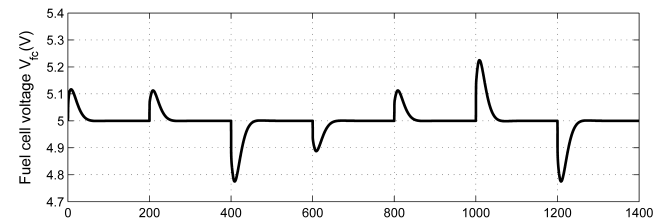
All the experimental tests were performed at the Fuel Cells Laboratory of the Institut de Robòtica i Informàtica Industrial (CSIC-UPC, Barcelona) and the authors would like to thank to the proficient technical staff. This research have been supported by ANPCyT (PICT project 2009-0017),

REFERENCES

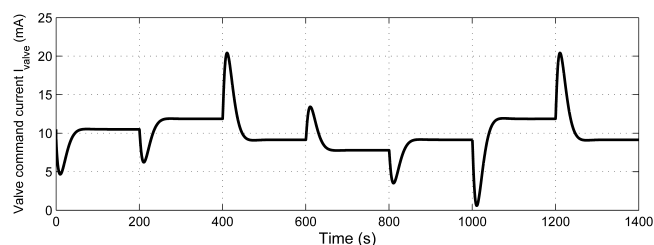
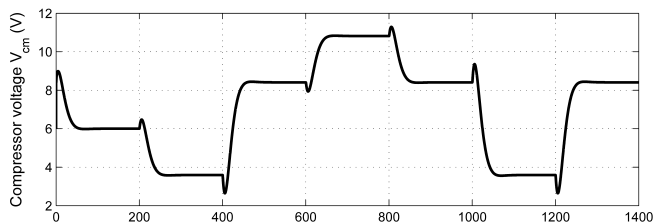
- [1] J. Pukrushpan, H. Peng, A. Stefanopoulou, Control-Oriented Modelling and Analysis for Automotive Fuel Cell Systems, *J. of Dynamic Systems*, vol. 126, 2004, pp 14-25.
- [2] D. Feroldi, M. Serra, J. Riera, Performance improvement of a PEMFC system controlling the cathode outlet air flow, *J. of Power Sources*, vol. 169, 2007, pp 205-212.
- [3] A. Niknezhadi, M. Allué-Fantova, C. Kunusch, C. Ocampo-Martínez, Design and implementation of LQR/LQG strategies for oxygen stoichiometry control in PEM fuel cells based systems, *J. of Power Sources*, vol. 196, 2010, pp 4277-4282.
- [4] J. Golbert and D. Lewin, Model-Based Control of Fuel Cells: (1) Regulatory Control, *J. of Power Sources*, vol. 135, 2004, pp 135-151.
- [5] M. Grujicic, K. Chittajallu, E. Law, J. Pukrushpan, Model-based control strategies in the dynamic interaction of air supply and fuel cell, *Proceedings of the Institution of Mechanical Engineers, Part A: J. of Power and Energy*, 218, 2004, pp 487-499.
- [6] D. Zumofen and M. Basualdo, Advanced control for fuel cells connected to a DC/DC converter and an electric motor, *Computer & Chemical Engineering*, vol. 34, pp 643-655, 2010.
- [7] Lucas Nieto Degliuomini, David Zumoffen Marta Basualdo, Diego Feroldi, Jordi Riera, Adaptive Predictive Robust Control for Fuel Cells Hybrid Vehicles, in *Vehicle Power and Propulsion Conference IEEE VPPC*, Lille, France, 2010, pp 4720-4729.
- [8] K. Yao, K. Karan, K. McAuley, P. Oosthuizen, B. Peppley, T. Xie, A Review of Mathematical Models for Hydrogen and Direct Methanol Polymer Electrolyte Membrane Fuel Cells, *Fuel Cells*, vol. 4, 2004, pp 3-29.
- [9] J. Amphlett, R. Mann, B. Peppley, P. Roberge, A. Rodrigues, A model predicting transient responses of proton exchange membrane fuel cells, *J. of Power Sources*, vol. 61, 1996, pp 183-188.
- [10] P.T. Nguyen, T. Berning, N. Djilali, Computational model of a PEM fuel cell with serpentine gas flow channels, *J. of Power Sources*, vol. 130, 2004, pp 149-157.
- [11] J.M. Maciejowski, *Predictive Control: With Constraints*, Prentice Hall, Englewood Cliffs, NJ; 2002.
- [12] A. Khadi-Sedig and B. Moaveni, *Control Configuration Selection for Multivariable Plants*, Editors: M. Thoma, F. Allgöwer, M. Morari, Springer-Verlag, UK, 2009.
- [13] G. Molina, D. Zumoffen, M. Basualdo, Plant-wide Control Strategy applied to the Tennessee Eastman Process at Two Operating Points, *Computer & Chemical Engineering*, vol. 35, pp 2081-2097, 2011.
- [14] E. Camacho and C. Bordons, *Model Predictive Control*, Springer-Verlag, UK; 1999.



(a) Disturbance profile of the fuel cell stack current.



(b) Controlled variables (oxygen excess ratio and fuel cell stack voltage).



(c) Manipulated variables (compressor motor voltage and cathode output valve current).

Fig. 7. Simulation results with DMC using the experimental step model.